Nonlinear Dynamics Emerging in Large Scale Neural Networks with Ontogenetic and Epigenetic Processes

Javier Iglesias, Olga K. Chibirova, and Alessandro E.P. Villa

Grenoble Institut des Neurosciences-GIN, Centre de Recherche
Inserm U 836-UJF-CEA-CHU
NeuroHeuristic Research Group, University Joseph Fourier, Grenoble, France
{Javier.Iglesias, Olga.Chibirova, Alessandro.Villa}@ujf-grenoble.fr
http://www.neuroheuristic.org/

Abstract. We simulated a large scale spiking neural network characterized by an initial developmental phase featuring cell death driven by an excessive firing rate, followed by the onset of spike-timing-dependent synaptic plasticity (STDP), driven by spatiotemporal patterns of stimulation. The network activity stabilized such that recurrent preferred firing sequences appeared along the STDP phase. The analysis of the statistical properties of these patterns give hints to the hypothesis that a neural network may be characterized by a particular state of an underlying dynamical system that produces recurrent firing patterns.

1 Introduction

The adult pattern of neuronal connectivity in the cerebral cortex is determined by the expression of genetic information, developmental differentiation and by epigenetic processes associated to plasticity and learning. During the early stages of development, excessive branches and synapses are initially formed and distributed somewhat diffusely (Innocenti, 1995). This over-growth phase is generally followed by massive synaptic pruning (Rakic et al., 1986) of only a selected subset of the connections initially established by a neuron. Trigger signals able to induce selective synaptic pruning could be associated to patterns of activity that depend on the timing of action potentials (Catalano and Shatz, 1998). Spike timing dependent synaptic plasticity (STDP) is a change in the synaptic strength based on the ordering of pre- and post-synaptic spikes. It has been proposed as a mechanism to explain the reinforcement of synapses repeatedly activated shortly before the occurrence of a post-synaptic spike (Bell et al., 1997). An equivalent mechanism is keen to explain the weakening of synapses strength whenever the pre-synaptic cell is repeatedly activated shortly after the occurrence of a post-synaptic spike (Karmarkar and Buonomano, 2002).

The study of the relation between synaptic efficacy and synaptic pruning suggests that the weak synapses may be modified and removed through competitive "learning" rules (Chechik et al., 1999). Despite the plasticity of these

J. Marques de Sá et al. (Eds.): ICANN 2007, Part I, LNCS 4668, pp. 579–588, 2007.
© Springer-Verlag Berlin Heidelberg 2007

phenomena it is rationale to suppose that whenever the same information is presented in the network the same pattern of activity is evoked in a circuit of functionally interconnected neurons, referred to as "cell assembly". Cell assemblies interconnected in this way would be characterized by recurrent, above chance levels, ordered sequences of precise (in the order of few ms) interspike intervals referred to as spatiotemporal patterns of discharges or preferred firing sequences (Abeles, 1991). Such precise firing patterns have been associated with specific behavioral processes in rats (Villa et al., 1999) and primates (Shmiel et al., 2006). Precise firing patterns have also been associated to deterministic nonlinear dynamics (Villa, 2000) and their detection in noisy time series could be performed by selected algorithms (Tetko and Villa, 1997; Asai et al., 2006).

In the current study we assume that developmental and/or learning processes are likely to potentiate or weaken certain pathways through the network and let emerge cell assemblies characterized by recurrent firing patterns. We investigate whether or not deterministic dynamics can be observed in the activity of a network by the analysis of the preferred firing sequences. The rationale is that a certain network, here identified by the simulation run, may be characterized by a particular state of an underlying dynamical system that produces recurrent firing patterns.

2 Neural Network Model

The complete neural network model is described in details elsewhere (Iglesias, Eriksson, Grize, Tomassini and Villa, 2005). A sketch description of the model with specific model parameters related to the current study follows below.

We assume that at time zero of the simulation the network is characterized by two types of integrate-and-fire units and by its maximum over growth in terms of connectivity. The total amount of units is 10,000 (8,000 excitatory and 2,000 inhibitory) laid down on a 100×100 2D lattice according to a space-filling quasi-random Sobol distribution. Two sets of 400 excitatory units (i.e., 800 units overall) were randomly selected among the 8,000 excitatory units of the network. The units belonging to these sets are the "sensory units" of the network, meaning that in addition to sending and receiving connections from the other units of both types they receive an input from the external stimulus.

The model features cell death mechanisms that may be provoked by: (i) an excessive firing rate and (ii) the loss of all excitatory inputs. An excessive firing rate is assumed to correspond to the biological effect known as glutamate neurotoxicity (Choi, 1988). During an initial phase called "early developmental phase", at each time step and for each unit a maximum firing rate was arbitrarily determined following a parameter search procedure described in (Iglesias and Villa, 2006). Whenever the rate of discharges of a unit exceeds the maximum allowed rate the cell had a probability to die according to a "genetically" determined probability function. A dead unit is characterized by the absence of any spiking activity.

At the end of the early developmental phase, the synaptic plasticity (Iglesias, Eriksson, Pardo, Tomassini and Villa, 2005) is enabled. It is assumed *a priori* that modifiable synapses are characterized by discrete activation levels (Montgomery and Madison, 2004) that could be interpreted as a combination of two factors: the number of synaptic *boutons* between the pre- and post-synaptic units and the changes in synaptic conductance. In the current study we attributed a fixed activation level (meaning no synaptic modification) $A_{ji}(t) = 1$, to *(inh, exc)* and *(inh, inh)* synapses while activation levels were allowed to take one of $A_{ji}(t) = \{0, 1, 2, 4\}$ for *(exc, exc)* and *(exc, inh)*, $A_{ji}(t) = 0$ meaning that the projection was permanently pruned out. For $A_{ji}(t) = 1$, the post-synaptic potentials were set to 0.84 mV and -0.8 mV for excitatory and inhibitory units, respectively. The projections from and to "dead" units undergo a decay of their synapses leading eventually to their pruning when $A_{ji}(t) = 0$. Other projections may be pruned due to synaptic depression driven by STDP and also leading to $A_{ji}(t) = 0$. Thus, some units that survived the early phase can also remain without any excitatory input. The loss of all excitatory inputs also provokes the cell death and these units stop firing (even in presence of background activity) immediately after the pruning of the last excitatory afference from within the network.

Two sets of 400 "sensory units" are stimulated by patterned activity organized both in time and space described elsewhere (Iglesias and Villa, 2006). This stimulus is assumed to correspond to content-related activity generated elsewhere in the brain. The overall stimulus duration is set to 100 ms, followed by a period without stimulation that lasted 1900 ms. Thus, the rate of stimulation was 0.5 $stim/s$.

3 Simulations

The values of the set of parameters specified above were kept constant throughout all this study. Because of a high sensitivity to the initial conditions of the pattern of connectivity we repeated the very same analysis with 30 different random generator seeds. Thus, each different seed generated a different connectivity (although keeping the same rules), different stimulus patterns and spontaneous activity patterns. Each simulation run lasted 10^5 discrete time steps (T_{end}), with 1 time step corresponding to 1 ms in the model, that means $100,000$ ms as total duration of a simulation run. The states (spiking/not spiking) of all units were updated synchronously. After spiking, the membrane potential was reset to its resting potential, and the unit entered an absolute refractory period lasting 3 and 2 time steps for excitatory and inhibitory units, respectively. Starting at time zero and throughout all the simulation run each unit received a background activity following an independent Poisson process of 5 $spikes/s$ on average.

The early developmental phase, characterized by cell death provoked by excessive firing rate, begins at time $t = 0$ and lasts until $t = T_{edp}$, that was fixed at 700 ms for this study. The spike timing dependent plasticity is enabled at $t = T_{edp} + 1$. At time $t = 1001$ ms the first stimulation is applied, lasting 100 ms

until $t = 1100\ ms$. Between $t = 1101\ ms$ and $t = 3000\ ms$ only the background activity is getting into the network. At time $t = 3001\ ms$ another stimulation is applied and so forth until the end of the simulation run. Overall this corresponds to 50 presentations of the stimulus along one simulation run.

The events belonging to the univariate time series corresponding to the spike train may have two different origins. Spikes may be simply associated to the Poisson background noise whenever the cell excitability is high and close enough to the threshold of activation. The other spikes can be produced by the convergence of synchronous activity (i.e., temporal summation of excitatory postsynaptic potentials) generated within the network. In order to study the time series of the spikes associated to the network activity those spikes associated to the background process were discarded from the spike trains and the so-called "effective spike trains" were extracted (Hill and Villa, 1997). Such effective spike trains were searched for the occurrence of spatiotemporal firing patterns, also called preferred firing sequences, by means of the "pattern grouping algorithm" (PGA) (Tetko and Villa, 2001). For the present study PGA was set to find patterns formed by three (triplets) or four spikes (quadruplets), with a significance level $p = 0.10$, provided the entire pattern did not last more than 800 ms and was repeated with a jitter accuracy of $\pm 5\ ms$.

All occurrences of all patterns detected by PGA within the same simulation run were merged together even if they were found in different units. This operation is aimed at detecting a possible underlying dynamical system that is associated to a specific network, thus encompassing the activity of several units belonging to the functional cell assembly. Such particular time series is referred to as "network patterned spike train", NP-spike train.

4 Results

At time $t = T_{end} = 100,000\ ms$ the units characterized by more than four active excitatory input projections that did not belong to the sets of "sensory units" were selected and their effective spike trains were analyzed. In one out of the 30 simulations, no spatiotemporal firing patterns could be found. In the other 29 simulations, 147 spatiotemporal firing patterns were detected, corresponding to 5672 spikes distributed into 61 triplets and 86 quadruplets. A single pattern could repeat between 5 (the minimum rate set in the algorithm) and 185 times. The vast majority of the patterns were composed by events belonging to the same neuron. We found only 3 triplets and 2 quadruplets composed by spikes produced by two different units.

Figure 1 illustrate two examples of patterns detected in the simulation run $S008$. The pattern $< 23E5, 23E5, 23E5\ ;\ 154 \pm 3.5, 364 \pm 3.0 >$ was composed by spikes produced by one unit labeled here #23E5 (Fig. 1a). This notation means that the pattern starts with a spike of unit $\#23E5$, followed $154 \pm 3.5\ ms$ later by a second spike of the same unit, and followed by a third spike $364 \pm 3.0\ ms$ after the pattern onset. We observed 15 repetitions of this pattern during the whole simulation run, but their occurrence was limited to the first half of the

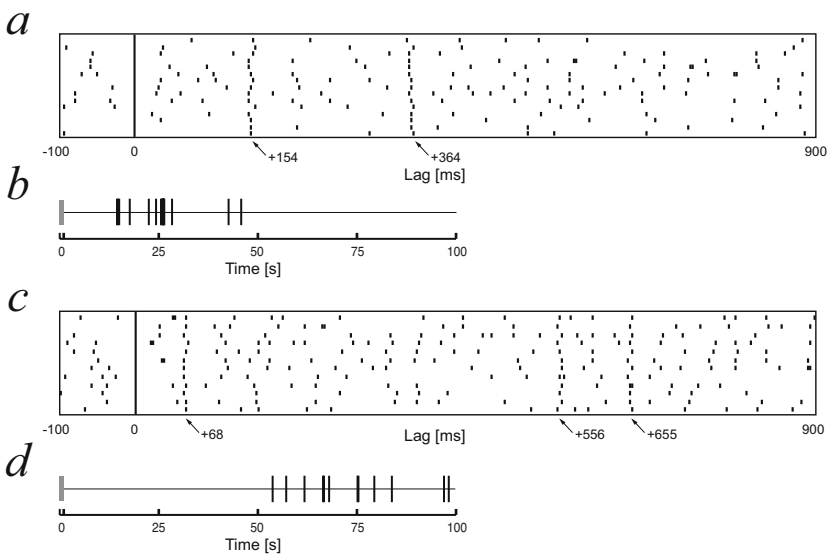

Fig. 1. **(a)**: Spatiotemporal pattern $< 23E5, 23E5, 23E5 \; ; \; 154 \pm 3.5, 364 \pm 3.0 >$. Raster plot showing 15 repetitions of the pattern aligned on the pattern start; **(b)**: Pattern occurrence timing plot of pattern (a) : each vertical tick represents the timing of the pattern onset; **(c)**: Spatiotemporal pattern $< B9B, B9B, B9B, B9B \; ; \; 68 \pm 2.0, 556 \pm 1.0, 655 \pm 4.0 >$ Raster plot showing 12 repetitions of the pattern aligned on the pattern start; **(d)**: Pattern occurrence timing plot of pattern (c)

simulation, and in particular in the period $[15-28]$ *seconds* (Fig. 1b). No correlation could be found between the timing of the spatiotemporal pattern and the stimulation onset. Figure 1c shows the occurrences of another pattern observed in the same network. This pattern labeled as $< B9B, B9B, B9B, B9B \; ; \; 68 \pm 2.0, 556 \pm 1.0, 655 \pm 4.0 >$ corresponds to a quadruplet that occurred only during the second half of the simulation.

Figure 2 shows the distribution of the onset times of all 147 patterns along the simulation duration. This histogram shows that patterns could start any time after the simulation onset. However, the majority of the patterns tended to appear and repeat above chance levels only during specific periods of the network life, thus suggesting the possibility of shifts in the temporally organized dynamics.

We investigated the distribution of the intra-pattern intervals, corresponding to the interval between the first and second event of the pattern (Figure 3a) and between the second and third event of the pattern (Figure 3b). In the case of quadruplets the intervals of the corresponding sub-patterns (the triplets) were considered for this analysis.

After detecting all patterns the NP-spike trains were constructed for each simulation run. In 19/30 simulation runs we found at least 4 different patterns, each of them repeating many times (Table 1). In these cases it appeared interesting to analyze the patterns that overlapped each other. For each pattern,

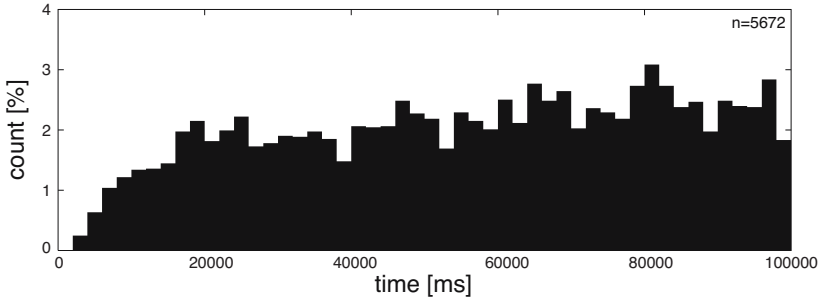

Fig. 2. Relative histogram of the onset time of all 147 patterns. Bin size: 2000 ms.

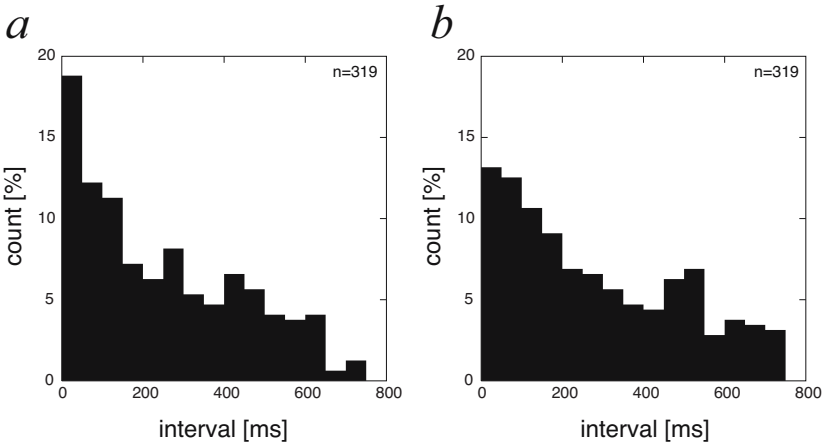

Fig. 3. Normalized distribution of the intervals among the triplets and quadruplets spikes. (***a***): intervals between the first and the second spike; (***b***): intervals between the second and the third spike. Bin size: 50 ms.

an overlapping factor was calculated to describe the probability for a pattern occurrence to overlap another occurrence from the same (self-overlap) or a different (cross-overlap) pattern. The number of overlaps o_i of each pattern i was incremented each time the onset spike of the jth pattern appeared between the first and the last spike of ith pattern. Then, for each kth network (i.e., for each simulation run), the normalized overlapping factor O_k was calculated as follows:

$$O_k = \frac{\sqrt{\sum o_i}}{n_k} \tag{1}$$

where o_i is the number of overlaps for each pattern i and n_k is the total number of occurrences for all the patterns found in the kth network. Table 1 shows that on average the overlapping factor was higher in the networks characterized by

Table 1. 147 patterns were observed in the activity of $N_{TOT} = 30$ distinct networks. Networks are arbitrarily divided into four classes clusterized by the number of different patterns found in each one. *Class 1*: less than 4 patterns; *Class 2*: between 4 an 6 patterns; *Class 3*: between 7 an 9 patterns; *Class 4*: at least 10 patterns. N: number of networks; $\hat{O}$: average overlapping factor for each class; $\hat{R}$: average number of pattern repetitions.

	N	$\widehat{O}$	$\widehat{R}$
Class 1	11	0.04	57.5
Class 2	13	0.06	41.0
Class 3	3	0.08	17.2
Class 4	3	0.07	33.8

7 to 9 different patterns. However, this result should not be considered too strongly because many more simulation runs are needed in order to extract significant statistical information.

The network $S008$ belonging to Class 3 was selected for the plot of the consecutive interspike intervals. Return maps correspond to the plots of the nth interspike-interval against the $(n-1)^{th}$ interspike-interval. Figure 4 shows, for two different time scales, the return map computed on the simulation NP-spike train as scatter plots (fig. 4a,b) and trajectories (fig. 4c,d). Notice the appearance of an ordered structure in the panels with scales $[0-250]$ ms (fig. 4b,d).

5 Discussion

We simulated a large scale spiking neural network, with the time resolution of 1 ms, characterized by a brief initial phase of cell death (Iglesias and Villa, 2006). The addition of this feature greatly improved the stability of the network while maintaining its ability to produce spatiotemporal firing patterns as shown in this study. During this phase the units that exceeded a certain threshold of firing had an increasing probability to die with the passing of time until 700 time units. After the stop of the massive cell death, spike timing dependent plasticity (STDP) and synaptic pruning were made active. Selected sets of units were activated by regular repetitions of a spatiotemporal pattern of stimulation. During the STDP phase, the cell death could occur only if a unit became deafferented, i.e. it lost all its excitatory afferences because of synaptic pruning.

We recorded the spike trains of all excitatory units that were not directly stimulated and that were surviving at the arbitrary end of the simulation set at $t = 100$ *seconds*. In these spike trains we searched for preferred firing sequences that occurred beyond random expectation (Tetko and Villa, 2001). We found 147 patterns in 30 different network configurations determined by different random seeds. It is interesting to notice that the effect of the initialization is important because only 6/30 networks were characterized by at least 7 detectable firing patterns. Moreover, we often observed patterns that occurred only during a limited time of the network life, usually in the order of 30 to 50 *seconds*. Such

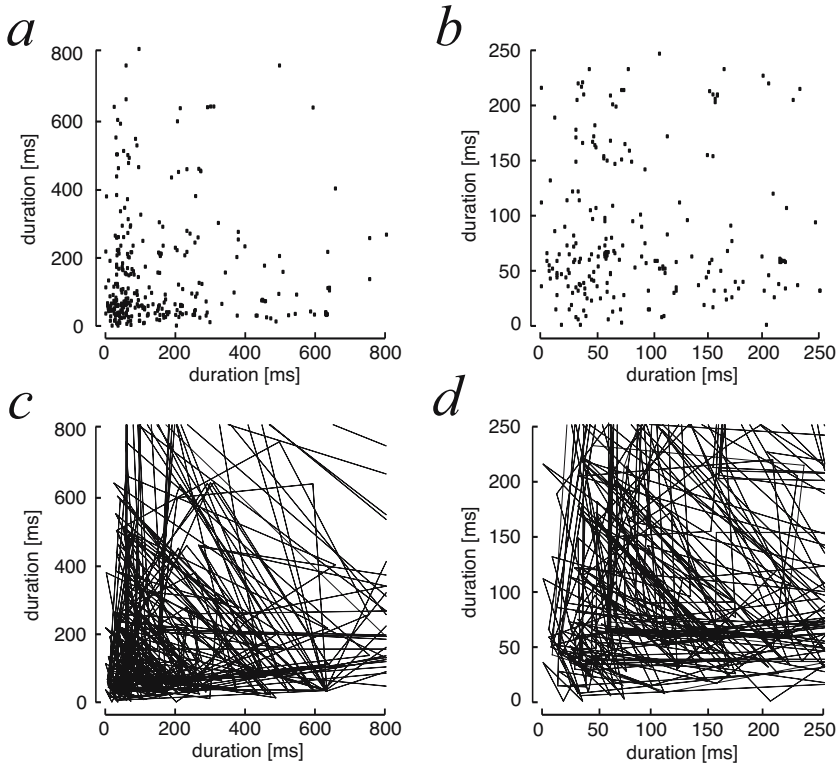

Fig. 4. Fingerprint of the dynamical activity of network $S008$ characterized by an overlapping factor equal to 0.09. $(\boldsymbol{a})$: Return map computed for intervals between $(\boldsymbol{a})$ 0 and 800 ms and $(\boldsymbol{b})$ focusing around 0 and 250 ms; $(\boldsymbol{c},\boldsymbol{d})$: Trajectories for the same data and intervals.

an example is illustrated by onset dynamics of the two patterns of Fig. 1. This observation might suggest that the network dynamics giving rise to a pattern occurrence may be suddenly disrupted by the continuous STDP-driven pruning. However, there is an extended overlap between patterns occurrence as shown by the overlapping factor described in this study. The process of patterns appearance looks more like a pattern giving the hand to another pattern but keeping the transition rather smooth.

The results presented here give some hints to the hypothesis that an underlying deterministic dynamical system, detected by the observation of an excess of preferred firing sequences, may appear under the drive of differentiation and learning processes. The fingerprints of the system observed in the return maps are suggestive of the presence of attractors and closed loops (Fig. 4). We believe that the current study opens new perspectives in this investigation but we are

aware of the necessity of future studies before any firm conclusion on the relations between preferred firing sequences and deterministic nonlinear dynamical systems.

Acknowledgments. This work was partially funded by the European Community Future and Emerging Technologies Complex Systems program, grant #034632 (PERPLEXUS), and New and Emerging Science and Technology program, grant #043309 (GABA).

References

Abeles, M.: Corticonics: Neural Circuits of the Cerebral Cortex, 1st edn. Cambridge University Press, Cambridge (1991)

Asai, Y., Yokoi, T., Villa, A.E.P.: Detection of a dynamical system attractor from spike train analysis. In: Kollias, S., Stafylopatis, A., Duch, W., Oja, E. (eds.) ICANN 2006. LNCS, vol. 4131, pp. 623–631. Springer, Heidelberg (2006)

Bell, C.C., Han, V.Z., Sugawara, Y., Grant, K.: Synaptic plasticity in a cerebellum-like structure depends on temporal order. Nature 387(6630), 278–281 (1997)

Catalano, S.M., Shatz, C.J.: Activity-dependent cortical target selection by thalamic axons. Science 281(5376), 559–562 (1998)

Chechik, G., Meilijson, I., Ruppin, E.: Neuronal regulation: A mechanism for synaptic pruning during brain maturation. Neural Computation 11, 2061–2080 (1999)

Choi, D.W.: Glutamate neurotoxicity and diseases of the nervous system. Neuron 1(8), 623–634 (1988)

Hill, S., Villa, A.E.: Dynamic transitions in global network activity influenced by the balance of excitation and inhibtion. Network: computational neural networks 8, 165–184 (1997)

Iglesias, J., Eriksson, J., Grize, F., Tomassini, M., Villa, A.E.: Dynamics of pruning in simulated large-scale spiking neural networks. BioSystems 79(1), 11–20 (2005)

Iglesias, J., Eriksson, J., Pardo, B., Tomassini, M., Villa, A.E.: Emergence of oriented cell assemblies associated with spike-timing-dependent plasticity. In: Duch, W., Kacprzyk, J., Oja, E., Zadrożny, S. (eds.) ICANN 2005. LNCS, vol. 3696, pp. 127–132. Springer, Heidelberg (2005)

Iglesias, J., Villa, A.: Neuronal cell death and synaptic pruning driven by spike-timing dependent plasticity. In: Kollias, S., Stafylopatis, A., Duch, W., Oja, E. (eds.) ICANN 2006. LNCS, vol. 4131, pp. 953–962. Springer, Heidelberg (2006)

Innocenti, G.M.: Exuberant development of connections, and its possible permissive role in cortical evolution. Trends in Neurosciences 18(9), 397–402 (1995)

Karmarkar, U.R., Buonomano, D.V.: A model of spike-timing dependent plasticity: one or two coincidence detectors? J. Neurophysiol. 88(1), 507–513 (2002)

Montgomery, J.M., Madison, D.V.: Discrete synaptic states define a major mechanism of synapse plasticity. Trends in Neurosciences 27(12), 744–750 (2004)

Rakic, P., Bourgeois, J., Eckenhoff, M.F., Zecevic, N., Goldman-Rakic, P.S.: Concurrent overproduction of synapses in diverse regions of the primate cerebral cortex. Science 232(4747), 232–235 (1986)

Shmiel, T., Drori, R., Shmiel, O., Ben-Shaul, Y.: Temporally precise cortical firing patterns are associated with distinct action segments. Journal of Neurophysiology 96(5), 2645–2652 (2006)

Tetko, I.V., Villa, A.E.: A comparative study of pattern detection algorithm and dynamical system approach using simulated spike trains. In: Gerstner, W., Hasler, M., Germond, A., Nicoud, J.-D. (eds.) ICANN 1997. LNCS, vol. 1327, pp. 37–42. Springer, Heidelberg (1997)

Tetko, I.V., Villa, A.E.: A pattern grouping algorithm for analysis of spatiotemporal patterns in neuronal spike trains. 1. detection of repeated patterns. Journal of Neuroscience Methods 105, 1–14 (2001)

Villa, A.E.: Time and the Brain. vol. 2. Harwood Academic Publishers (2000)

Villa, A.E., Tetko, I., Hyland, B., Najem, A.: Spatiotemporal activity patterns of rat cortical neurons predict responses in a conditioned task. Proc. Natl. Acad. Sci. USA 96, 1106–1111 (1999)